AAS 10-210

American Astronautical Society

American Institute of Aeronautics and Astronautics

TWO-CRAFT COULOMB FORMATION RELATIVE EQUILIBRIA ABOUT CIRCULAR ORBITS AND LIBRATION POINTS

Ravi Inampudi and Hanspeter Schaub

AAS/AIAA Space Flight Mechanics Conference

San Diego, California August 14–18, 2010

AAS Publications Office, P.O. Box 28130, San Diego, CA 92198

AAS 10-210

TWO-CRAFT COULOMB FORMATION RELATIVE EQUILIBRIA ABOUT CIRCULAR ORBITS AND LIBRATION POINTS

Ravi Inampudi* **and Hanspeter Schaub**†

The charged relative equilibria of a two spacecraft Coulomb formation moving in the context of a restricted two-body system and a circularly restricted three-body system are investigated. For a two-spacecraft formation moving in a central gravitational field it is often assumed that the center of the circular orbit is located at the primary mass, and the center of mass of the formation orbits around the primary in a great circle orbit. The relative equilibrium is called great circle if the center of mass of the formation moves on the plane with the center of the gravitational field residing on it; otherwise, it is called a non-great-circle orbit. Previous research shows that non-great-circle equilibria in low Earth orbits, have a deflection from the great circle equilibria of about a degree when spacecraft with unequal masses are separated by 350 km. This paper investigates these equilibria (radial, tangential and orbit normal in circular Earth orbit and Earth-Moon Libration points) in the context of two spacecraft Coulomb formation, and shows that the equilibria deflections are negligible (on the order of 10^{-6} degrees) even for very heterogeneous mass distributions. Further, the non-great-circle equilibria conditions for a two-spacecraft virtual Coulomb structure at the Lagrangian Libration points are developed. The development is based on exact gravitational and Coulomb potentials and considers the effect of mass asymmetry of the formation in the problem formulation.

INTRODUCTION

This paper discusses the relative equilibria of two masses virtually connected by an electrostatic (Coulomb) force moving in the presence of a central gravitational force field as well as the relative equilibria of the Coulomb formation at the libration points moving around the barycenter. This novel method of exploiting Coulomb forces for formation flying control with separation distance on the order of dozens of meters was introduced in References.[1,2] Since then, there has been many interesting investigations on dynamics and control problems of Coulomb formation.[3,4,10,11,12,13] In particular, References 6, 7, 8 and 9 study static Coulomb structures where the differential gravitational forces between spacecraft are canceled through constant electrostatic forces. Thus, the open-loop equilibrium charges cause the virtual structure to assume a constant shape as seen by the rotating orbit frame. The Coulomb tether formation has several potential applications in space technologies, for example, high accuracy wide-field-of-view optical interferometry missions with geostationary orbits (GEO), spacecraft cluster control, as well as deployment or retrieval of dedicated sensors using Coulomb forces.

In the context of a restricted two-body problem existence of great circle relative equilibria for a satellite system implies that the center of the circular orbit coincides with the center of the gravitational field. If the satellite is assumed to be a rigid body, and making a first order approximation

*Graduate Student, Aerospace Engineering Sciences Department, University of Colorado, Boulder, CO.
†Associate Professor, H. Joseph Smead Fellow, Aerospace Engineering Sciences Department, University of Colorado, Boulder, CO.

of the gravitational force acting on the rigid body as well as assuming that the orbital motion is decoupled from the attitude motion, the classical rigid-body attitude equilibrium study yields that all three rigid body principal axes must line up with the LVLH (Local vertical/local horizontal) frame axes. However, References 14 and 15 prove the existence of non-great-circle relative equilibria of rigid bodies where the center of mass of the circular orbit traces a cone rather than a disk around the center of the gravitational field. Here the exact potential function expression is used in their analysis, and large variations in orientation from the classic regular motions are verified analytically and numerically. The orientation change between great-circle and non-great-circles solutions is particularly noticeable if the mass distribution of the rigid body is as asymmetric as possible.

In a three-body system we consider a spacecraft formation near two large celestial objects who are rotating around their common center of mass. Due to the rotation of the system, there are five equilibrium points; these equilibrium points are the libration points (L_1-L_5) of the three-body system. Virtual Coulomb structures at the libration points are useful for remote-sensing missions to establish a long baseline imaging capability, or to ensure better stationkeeping configurations. Reference 17 considers the equilibrium configurations of a rigid tethered system near all five libration points and carries out the stability analysis when it is near the translunar libration point.

Reference 15 discusses the relative equilibria and relative stability of a system of two spring-connected point masses moving in a central gravitational field. The paper shows that non-great-circle equilibria exist for this simple spring system, and, for long tethers of approximately 3500 km at LEO the attitude deflection from the vertical can reach tens of degrees. Also, the effect of mass asymmetry of the formation on the non-great-circle relative equilibria is studied. In order to gain further insights on the effects of non-great-circle relative equilibria and mass asymmetry on a two spacecraft formation the tether is modeled using a Coulomb force in this paper. The goal is to analytically derive the great circle relative equilibria of a two spacecraft Coulomb formation in a restricted two body system, and use this methodology to derive new 2-craft virtual Coulomb structure condition for a restricted three body system. Therefore, an exact model for the gravitational and Coulomb potential is used to compute the relative equilibria. Just as the spring system possesses $\boldsymbol{SO}(3)$ symmetry, the Coulomb formation has $\boldsymbol{SO}(3)$ symmetry. Such symmetry in geometric mechanics induces certain reduced dynamics which facilitates to get the conditions of relative equilibria. To obtain the conditions for relative equilibria, the principle of symmetric criticality is applied.[15] Moreover, the effects of non-great-circle relative equilibria and mass asymmetry on a two spacecraft formation as a function of spacecraft separation distances (short to long tethers) and formation center of mass distances from LEO to GEO, as well as in the context of a three body system are studied.

In this paper, the following assumptions are made

1. The Coulomb tether undergoes both tensile and compressive forces along the line-of-sight direction between the two spacecraft.
2. The gravitational attraction between the two spacecraft masses is neglected.
3. For the three-body system the spacecraft formation motion is in the plane of the motion of the primary bodies.

The objective of this paper is to study the relative equilibria of a two spacecraft static Coulomb structure using the exact gravitational and Coulomb potentials. The necessary conditions for a virtual Coulomb structure where the orbital motion is decoupled from the attitude motion are discussed in Reference 6. References 9, 11, 12 search for static Coulomb structure solutions using genetic algorithms. Here the simple principle axes condition of rigid body equilibria are used to speed up the genetic search algorithms. In this paper we are investigating the validity of this assumption for Coulomb tether applications taking non-great-circle equilibria conditions into account. The goal is to identify for what formation dimension and altitudes these non-great circle effects become significant. Further, for a two spacecraft Coulomb formation, this paper presents the relative equilibria for a three-body system at all five libration points.

The paper is organized as follows. The system dynamics and the notion of $\boldsymbol{SO}(3)$ symmetry applied to Coulomb formation moving in a central gravitational field as well as for a restricted three-body system are discussed. Then the principle of symmetric criticality is applied to determine the conditions of relative equilibria of charged static structures. For the restricted two-body system, the reduced dynamics identifies the classical great circle equilibria for the Coulomb formation; tangential, orbit normal and radial equilibria. Similar relative equilibria solutions are derived at for the libration points. Also, the non-great circle effects in circular orbits on any two spacecraft formation existing from low Earth orbits (LEO) to geostationary orbits (GEO) are investigated.

SYSTEM DESCRIPTION AND *SO(3)* SYMMETRY

In the following sections, we introduce the fundamental concepts related to the dynamics of a system of N spacecrafts moving in a central gravitational field (restricted two-body system) and moving under the mutual gravitation of two bodies (restricted three-body system).

Restricted Two-body System

The spacecrafts shown in the Figure 1 can be considered to be point masses moving in a central gravitational field. With the static virtual Coulomb structure the system of spacecrafts behaves equivalently to a rigid body in orbit because the constant electrostatic inter-spacecraft forces cancel perfectly the differential gravitational forces acting across the cluster. Let $\boldsymbol{F}_c$ be the Coulomb force acting between the two masses, and $\boldsymbol{r}_i$ be the inertial position vector of a single craft of mass m_i. Then the center of mass position vector $\boldsymbol{r}_c$ of this formation is defined as

$$\boldsymbol{r}_c = \frac{1}{M}\sum_{i=1}^{N} m_i \boldsymbol{r}_i \tag{1}$$

with $M = \sum_{i=1}^{N} m_i$ being the total formation mass. Let O be the center of the inverse square field and the origin of the inertial frame, while the formation's center of mass and center of gravity are denoted by C and G, respectively. The inertial position vectors of C and G are $\boldsymbol{r}_c$ and $\boldsymbol{r}_g$ and are related by

$$\boldsymbol{r}_g - \boldsymbol{r}_c = \boldsymbol{r} \tag{2}$$

where $\boldsymbol{r}$ is the constant vector between C and G.

From Newton's laws of gravitation the following relation relating the formation center of gravity and the individual inertial vectors is obtained as

$$\frac{\boldsymbol{r}_g}{\|\boldsymbol{r}_g\|^3} = \frac{1}{M}\sum_{i=1}^{N} \frac{\boldsymbol{r_i}}{\|\boldsymbol{r_i}\|^3} m_i \tag{3}$$

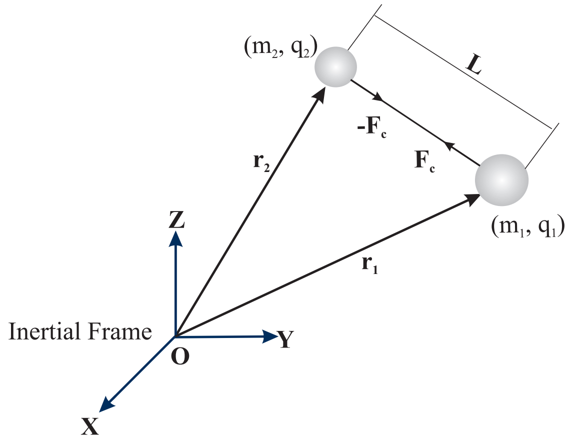

Figure 1. Two-Craft Coulomb Spacecraft Formation (Restricted Two-body System)

Using the two-body relative equations of motion with respect to G, the inertial second derivative of the vector $\boldsymbol{r}_g$ is

$$\frac{d^2\boldsymbol{r}_g(t)}{dt^2} + \frac{\mu \boldsymbol{r}_g(t)}{\|\boldsymbol{r}_g(t)\|^3} = 0 \tag{4}$$

Therefore, from Eqs. (2) and (4), the inertial second derivatives of the vectors $\boldsymbol{r}_c$ and $\boldsymbol{r}_g$ are related by

$$\frac{d^2\boldsymbol{r}_c(t)}{dt^2} + \frac{\mu \boldsymbol{r}_g(t)}{\|\boldsymbol{r}_g(t)\|^3} = 0 \tag{5}$$

Let m_1 and m_2 denote the mass of each craft with inertial position vectors $\boldsymbol{r_1}$ and $\boldsymbol{r_2}$, while each craft is assumed to have electrostatic (Coulomb) charges q_1 and q_2. The kinetic energy of the system is then given by

$$T(\dot{\boldsymbol{r}}_1, \dot{\boldsymbol{r}}_2) = \frac{m_1}{2}\|\dot{\boldsymbol{r}}_1\|^2 + \frac{m_2}{2}\|\dot{\boldsymbol{r}}_2\|^2 \tag{6}$$

The potential energy of the system is

$$V(\boldsymbol{r_1}, \boldsymbol{r_2}) = -\frac{\mu m_1}{\|\boldsymbol{r_1}\|} - \frac{\mu m_2}{\|\boldsymbol{r_2}\|} + k_c \frac{q_1 q_2}{\|\boldsymbol{r_1} - \boldsymbol{r_2}\|} e^{-\frac{\|\boldsymbol{r_1} - \boldsymbol{r_2}\|}{\lambda_d}} \tag{7}$$

The first two terms of the potential energy are the gravitational potential of each point mass in orbit about a planet with mass m and gravitational constant μ. The third term denotes the Coulomb potential energy generated by the two spacecrafts in a plasma environment where $k_c = 8.99 \times 10^9$ Nm^2/C^2 is the Coulomb's constant and $\|\boldsymbol{r_1} - \boldsymbol{r_2}\|$ is the separation distance between the two spacecrafts. The exponential term depends on the Debye length parameter λ_d which controls the electrostatic field strength of plasma shielding between the craft. At Geostationary Orbits (GEO) the Debye length vary between 80-1400 m, with a mean of about 180 m. The Coulomb spacecraft formation studied in this paper is assumed to be orbiting on high Earth orbits.

In this paper the relative equilibria of a formation with two spacecraft subjected to Coulomb forces is considered where there are no external forces acting on the system. The relative equilibrium of the spacecraft formation can be introduced by defining a uniformly rotating frame located at the origin O which has a constant orbital angular velocity of $\boldsymbol{\xi}$. A formation moving in a circular orbit that is stationary relative to this uniformly rotating frame exhibits symmetry with respect to the special orthogonal rotation group $\boldsymbol{SO}(3)$. $\boldsymbol{SO}(3)$ rotation group and other group theoretic concepts used in this paper are explained in are briefly explained in Appendix A.

For instance, the Coulomb formation has the $\boldsymbol{SO}(3)$ symmetry because the kinetic and potential energy are invariant under the $\boldsymbol{SO}(3)$ actions. This symmetry helps to reduce the dynamics by the $\boldsymbol{SO}(3)$ group action, and the equilibrium of the reduced dynamics is the relative equilibrium of the spacecraft formation. If the center of mass of the formation moves on a great-circle orbit, then the relative equilibrium is called the great-circle relative equilibrium. This implies that $\boldsymbol{r}_c \cdot \boldsymbol{\xi} = 0$; if $\boldsymbol{r}_c \cdot \boldsymbol{\xi} \neq 0$ it is called the nongreat-circle relative equilibrium[14] as shown in the Figure 2.

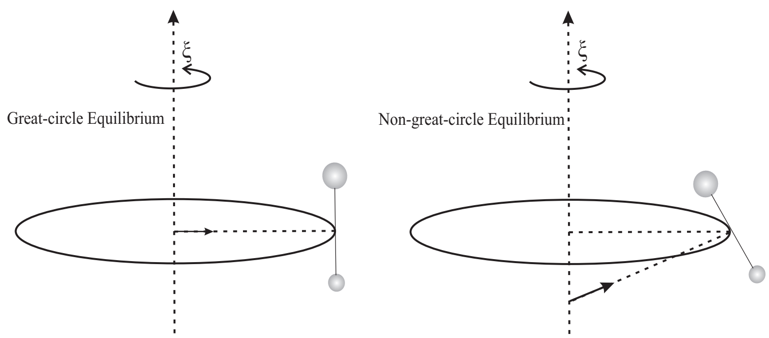

Figure 2. Two-Craft Coulomb Spacecraft Formation (Restricted Two-body System)

Using the properties of Lie algebra $\boldsymbol{g}^*$ of $\boldsymbol{SO}(3)$, at relative equilibria there exists two constant inertial vectors $\boldsymbol{r}_{co}$ and $\boldsymbol{r}_{go}$ with respect to O such that $\boldsymbol{r}_c(t) = e^{\hat{\boldsymbol{\xi}}t}\boldsymbol{r}_{co}$ and $\boldsymbol{r}_g(t) = e^{\hat{\boldsymbol{\xi}}t}\boldsymbol{r}_{go}$. Therefore at relative equilibrium Eq.(5) can be reduced to

$$\hat{\boldsymbol{\xi}}\hat{\boldsymbol{\xi}}\boldsymbol{r}_{co} + \frac{\mu \boldsymbol{r}_{go}}{\|\boldsymbol{r}_{go}\|^3} = 0 \tag{8}$$

Taking an inner product of Eq. (8) with $\boldsymbol{\xi}$ gives $\boldsymbol{r}_{go} \cdot \boldsymbol{\xi} = 0$. Consequently, at relative equilibria the center of gravity of a spacecraft formation moving in a central gravitational field traces a great circle.

Restricted Three-body System

In a three-body system, as shown in Figure 3, the spacecrafts are considered to be point masses moving around the barycenter O under the mutual gravitation of two bodies M_1 and M_2. The relative equilibrium of the spacecraft formation can be introduced by defining a uniformly rotating frame located at the barycenter O which has a constant orbital angular velocity of $\boldsymbol{\xi}$. A formation moving in a circular orbit that is stationary relative to this uniformly rotating frame exhibits symmetry with respect to $\boldsymbol{SO}(3)$. If m_1 and m_2 denote the mass of each craft with inertial position vectors $\boldsymbol{R}_{11}$, $\boldsymbol{R}_{12}$, $\boldsymbol{R}_{21}$ and $\boldsymbol{R}_{22}$ then using the three-body relative equations of motion, the inertial second derivative of the vector $\boldsymbol{r}_g$ is

$$M\ddot{\boldsymbol{r}}_g = -\mu_1\left(\frac{m_1}{R_{11}^3}\boldsymbol{R}_{11} + \frac{m_2}{R_{21}^3}\boldsymbol{R}_{21}\right) - \mu_2\left(\frac{m_1}{R_{12}^3}\boldsymbol{R}_{12} + \frac{m_2}{R_{22}^3}\boldsymbol{R}_{22}\right) \tag{9}$$

where M is the total formation mass, and μ_1 and μ_2 are the gravitational parameters of the two planets. The inertial position vectors $\boldsymbol{R}_{11}$, $\boldsymbol{R}_{12}$, $\boldsymbol{R}_{21}$ and $\boldsymbol{R}_{22}$ can be expressed in rotating coordi-

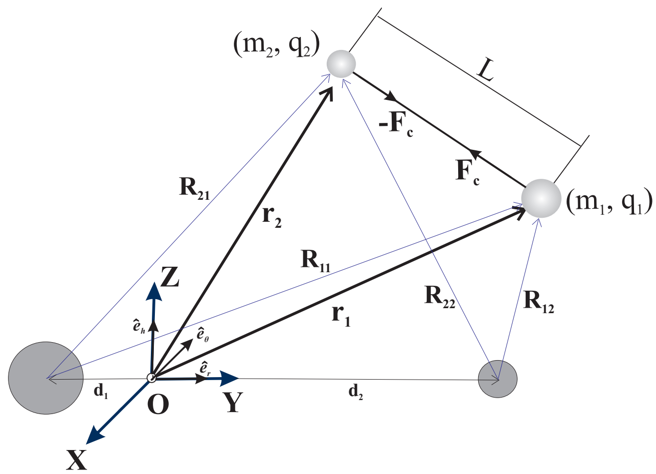

Figure 3. Two-Craft Coulomb Spacecraft Formation (Restricted Three-body System)

nates (synodic frame at the barycenter O) such that the distances are invariant under rotation. The synodic frame $S : \{\hat{\boldsymbol{e}}_r, \hat{\boldsymbol{e}}_\theta, \hat{\boldsymbol{e}}_h\}$ is rotating around the axis Oz with the constant angular velocity Ω defined as

$$\Omega = \sqrt{\frac{G\left(M_1 + M_2\right)}{d^3}} \tag{10}$$

where G is the gravity constant and d is the distance between the two planets. The primaries are at rest in the synodic frame at positions $M_1(-d_1, 0, 0)$ and $M_2(d_2, 0, 0)$. Also, if each craft with rotating position vectors $\boldsymbol{r_1}$ and $\boldsymbol{r_2}$ is assumed to have electrostatic (Coulomb) charges q_1 and q_2 then the kinetic energy of the system is still given by Eq. 6. However, the potential energy of the system becomes

$$\begin{aligned} V\left(\boldsymbol{r_1}, \boldsymbol{r_2}\right) = &-\mu_1 \left(\frac{m_1}{\|\boldsymbol{r_1} - \boldsymbol{d}_1\|} + \frac{m_2}{\|\boldsymbol{r_2} - \boldsymbol{d}_1\|}\right) - \mu_2 \left(\frac{m_1}{\|\boldsymbol{r_1} - \boldsymbol{d}_2\|} + \frac{m_2}{\|\boldsymbol{r_2} - \boldsymbol{d}_2\|}\right) \\ &+ k_c \frac{q_1 q_2}{\|\boldsymbol{r_1} - \boldsymbol{r_2}\|} e^{-\frac{\|\boldsymbol{r_1} - \boldsymbol{r_2}\|}{\lambda_d}} \end{aligned} \tag{11}$$

Since the kinetic and potential energy are invariant under the $\boldsymbol{SO}(3)$ actions, the Coulomb formation thus moving around the barycenter has the $\boldsymbol{SO}(3)$ symmetry. This symmetry helps in the reduced dynamics by the $\boldsymbol{SO}(3)$ group action and the equilibrium of the reduced dynamics is the relative equilibrium of the spacecraft formation in the three-body system. Therefore, similar to the definitions for a two-body system, in a three-body system $\boldsymbol{r}_c \cdot \boldsymbol{\xi} = 0$ implies that the center of mass of the formation moves on a great-circle orbit and hence the relative equilibrium is called the great-circle relative equilibrium. And, if $\boldsymbol{r}_c \cdot \boldsymbol{\xi} \neq 0$ it is called the nongreat-circle relative equilibrium.

RELATIVE EQUILIBRIA OF THE STATIC TWO-CRAFT COULOMB FORMATION

Since the static two-craft Coulomb formation has the $\boldsymbol{SO}(3)$ symmetry, the dynamics in the original phase space of the system can be reduced yielding the reduced dynamics. The relative equilibria of the reduced dynamics facilitates in finding the equilibrium configurations. Given a simple mechanical system with symmetry (Q,T,V,G), where Q is the configuration space with G-invariant Riemannian metric K on Q, T is the G-invariant kinetic energy and V is the G-invariant potential function, and G is the symmetry (Lie) group, then we have the following useful theorem based on the principle of symmetric criticality.[15]

$\boldsymbol{Theorem}$ **:** For a simple dynamical system with symmetry (Q,T,V,G) and the metric

$$K\left(\boldsymbol{q}\right)\left(\boldsymbol{v_q},\boldsymbol{v_q}\right)=2T\left(\boldsymbol{v_q}\right)\quad with\;\; \boldsymbol{v_q}\in TQ \tag{12}$$

define the augmented potential $V_\xi : Q \rightarrow \mathbf{R}$,

$$V_\xi\left(\boldsymbol{q}\right)=V\left(\boldsymbol{q}\right)-\frac{1}{2}K\left(\boldsymbol{q}\right)\left(\boldsymbol{\xi}_Q\left(\boldsymbol{q}\right),\boldsymbol{\xi}_Q\left(\boldsymbol{q}\right)\right) \tag{13}$$

where $\boldsymbol{\xi}_Q$ is the infinitesimal generator associated with $\boldsymbol{\xi}$. Then at relative equilibrium $\boldsymbol{q_e}$ is a critical point of V_ξ for some $\boldsymbol{\xi}\in\boldsymbol{g}^*$.

Therefore, for the two-craft Coulomb formation the *augmented* potential function V_ξ is

$$V_\xi\left(\boldsymbol{r_1},\boldsymbol{r_2}\right)=V\left(\boldsymbol{r_1},\boldsymbol{r_2}\right)-\frac{m_1}{2}\left\langle\boldsymbol{\xi}\times\boldsymbol{r_1},\boldsymbol{\xi}\times\boldsymbol{r_1}\right\rangle-\frac{m_2}{2}\left\langle\boldsymbol{\xi}\times\boldsymbol{r_2},\boldsymbol{\xi}\times\boldsymbol{r_2}\right\rangle \tag{14}$$

where $\boldsymbol{\xi}\in\mathbf{R^3}$ is an arbitrary constant vector. According to the principle of symmetric criticality, the relative equilibria corresponding to some $\boldsymbol{\xi}$ can be characterized by the critical points of the augmented potential V_ξ.

RELATIVE EQUILIBRIA IN THE RESTRICTED TWO-BODY SYSTEM

For the Coulomb spacecraft formation with $\boldsymbol{SO}(3)$ symmetry, the relative equilibrium is an equilibrium in a uniformly rotating frame. If the vector $\boldsymbol{\xi}$ denotes the angular velocity of the uniformly rotating frame, the augmented potential for the two spacecraft formation is,

$$\begin{aligned}V_\xi\left(\boldsymbol{r_1},\boldsymbol{r_2}\right)=&-\frac{\mu m_1}{\|\boldsymbol{r_1}\|}-\frac{\mu m_2}{\|\boldsymbol{r_2}\|}+k_c\frac{q_1q_2}{\|\boldsymbol{r_1}-\boldsymbol{r_2}\|}e^{-\frac{\|\boldsymbol{r_1}-\boldsymbol{r_2}\|}{\lambda_d}}\\&-\frac{m_1}{2}\left\langle\boldsymbol{\xi}\times\boldsymbol{r_1},\boldsymbol{\xi}\times\boldsymbol{r_1}\right\rangle-\frac{m_2}{2}\left\langle\boldsymbol{\xi}\times\boldsymbol{r_2},\boldsymbol{\xi}\times\boldsymbol{r_2}\right\rangle\end{aligned} \tag{15}$$

Then the relative equilibria of the system can be characterized by the critical points of the augmented potential V_ξ. The first variation of V_ξ taken component wise with respect to $\boldsymbol{q}=(\boldsymbol{r_1},\boldsymbol{r_2})$ is computed as

$$\begin{aligned}\boldsymbol{D}V_\xi\left(\boldsymbol{r_1},\boldsymbol{r_2}\right)\cdot\left(\delta\boldsymbol{r_1},\delta\boldsymbol{r_2}\right)=&\,\mu m_1\frac{\boldsymbol{r_1}}{\|\boldsymbol{r_1}\|^3}\cdot\delta\boldsymbol{r_1}+\mu m_2\frac{\boldsymbol{r_2}}{\|\boldsymbol{r_2}\|^3}\cdot\delta\boldsymbol{r_2}\\&-k_c\frac{q_1q_2}{\|\boldsymbol{r_1}-\boldsymbol{r_2}\|^2}e^{-\frac{\|\boldsymbol{r_1}-\boldsymbol{r_2}\|}{\lambda_d}}\left[1+\frac{\|\boldsymbol{r_1}-\boldsymbol{r_2}\|}{\lambda_d}\right]\frac{\boldsymbol{r_1}-\boldsymbol{r_2}}{\|\boldsymbol{r_1}-\boldsymbol{r_2}\|}\cdot\left(\delta\boldsymbol{r_1}-\delta\boldsymbol{r_2}\right)\\&+m_1\left(\hat{\boldsymbol{\xi}}\hat{\boldsymbol{\xi}}\boldsymbol{r_1}\right)\cdot\delta\boldsymbol{r_1}+m_2\left(\hat{\boldsymbol{\xi}}\hat{\boldsymbol{\xi}}\boldsymbol{r_2}\right)\cdot\delta\boldsymbol{r_2}\end{aligned} \tag{16}$$

Let $V_c^{'}$ denote the derivative of Coulomb potential with respect to $\|\boldsymbol{r_1}-\boldsymbol{r_2}\|$ which represents the Coulomb forces acting between the two crafts. Then $V_c^{'}$ is

$$V_c^{'}\left(\|\boldsymbol{r_1}-\boldsymbol{r_2}\|\right)=-k_c\frac{q_1q_2}{\|\boldsymbol{r_1}-\boldsymbol{r_2}\|^2}e^{-\frac{\|\boldsymbol{r_1}-\boldsymbol{r_2}\|}{\lambda_d}}\left[1+\frac{\|\boldsymbol{r_1}-\boldsymbol{r_2}\|}{\lambda_d}\right] \tag{17}$$

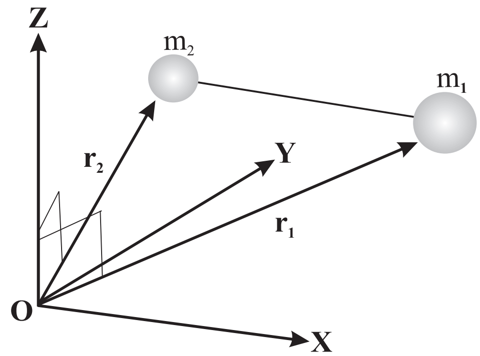

Figure 4. The Rotating Reference Frame

Then Eq. (16) is expressed as

$$
\begin{aligned}
DV_{\xi}\left(\boldsymbol{r_1},\boldsymbol{r_2}\right)\cdot\left(\delta\boldsymbol{r_1},\delta\boldsymbol{r_2}\right) &= \mu m_1 \frac{\boldsymbol{r_1}}{\|\boldsymbol{r_1}\|^3}\cdot\delta\boldsymbol{r_1} + \mu m_2 \frac{\boldsymbol{r_2}}{\|\boldsymbol{r_2}\|^3}\cdot\delta\boldsymbol{r_2} \\
&+ V_c^{'}\left(\|\boldsymbol{r_1}-\boldsymbol{r_2}\|\right)\frac{\boldsymbol{r_1}-\boldsymbol{r_2}}{\|\boldsymbol{r_1}-\boldsymbol{r_2}\|}\cdot\left(\delta\boldsymbol{r_1}-\delta\boldsymbol{r_2}\right) \qquad (18)\\
&+ m_1\left(\hat{\boldsymbol{\xi}}\hat{\boldsymbol{\xi}}\boldsymbol{r_1}\right)\cdot\delta\boldsymbol{r_1} + m_2\left(\hat{\boldsymbol{\xi}}\hat{\boldsymbol{\xi}}\boldsymbol{r_2}\right)\cdot\delta\boldsymbol{r_2}
\end{aligned}
$$

By setting $DV_{\xi}\left(\boldsymbol{r_{1e}},\boldsymbol{r_{2e}}\right)=0$ we arrive at the following conditions of relative equilibria:

$$
\frac{\mu m_1 \boldsymbol{r_{1e}}}{r_{1e}^3} + m_1\hat{\boldsymbol{\xi}}\hat{\boldsymbol{\xi}}\boldsymbol{r_{1e}} + V_c^{'}\frac{\boldsymbol{r_{1e}}-\boldsymbol{r_{2e}}}{\|\boldsymbol{r_{1e}}-\boldsymbol{r_{2e}}\|} = 0 \qquad (19a)
$$

$$
\frac{\mu m_2 \boldsymbol{r_{2e}}}{r_{2e}^3} + m_2\hat{\boldsymbol{\xi}}\hat{\boldsymbol{\xi}}\boldsymbol{r_{2e}} - V_c^{'}\frac{\boldsymbol{r_{1e}}-\boldsymbol{r_{2e}}}{\|\boldsymbol{r_{1e}}-\boldsymbol{r_{2e}}\|} = 0 \qquad (19b)
$$

where $r_{1e}=\|\boldsymbol{r_{1e}}\|$ and $r_{2e}=\|\boldsymbol{r_{2e}}\|$.

Now consider a rotation matrix $[RN]\in\boldsymbol{SO}(3)$ that maps vectors from an inertial frame N into a new reference frame R. If we denote the vectors $\boldsymbol{R_1}$, $\boldsymbol{R_2}$, $\boldsymbol{\omega}$ in the reference frame R then the conditions of relative equilibria given in Eqs. 19a and 19b are invariant under the transformation $\boldsymbol{R_1}=[RN]\,\boldsymbol{r_{1e}}$, $\boldsymbol{R_2}=[RN]\,\boldsymbol{r_{2e}}$ and $\boldsymbol{\omega}=[RN]\,\boldsymbol{\xi}$. In order to solve for relative equilibria, the new reference frame should be chosen such that the number of unknowns are at minimum in the equilibrium conditions. As illustrated in Figure 6(d), a reference frame is chosen such that the x-axis is parallel to the line connecting the two crafts, the z-axis being perpendicular to both the vectors $\boldsymbol{r_{1e}}$ and $\boldsymbol{r_{2e}}$, and the y-axis completing the triad.

In the context of the new frame R, the vectors can be expressed as $\boldsymbol{R}_1=(x_1,y_c,0)^T$, $\boldsymbol{R}_2=(x_2,y_c,0)^T$, and $\boldsymbol{\omega}=(\omega_1,\omega_2,\omega_3)^T$. Now the equilibrium conditions (19a) and (19b) expressed in scalar form are,

$$-\left(\omega_2^2+\omega_3^2\right)x_1+\omega_1\omega_2 y_c+\mu\frac{x_1}{R_1^3}=-\frac{V_c'}{m_1} \tag{20}$$

$$\omega_1\omega_2 x_1-\left(\omega_1^2+\omega_3^2\right)y_c+\mu\frac{y_c}{R_1^3}=0 \tag{21}$$

$$\left(\omega_1 x_1+\omega_2 y_c\right)\omega_3=0 \tag{22}$$

$$-\left(\omega_2^2+\omega_3^2\right)x_2+\omega_1\omega_2 y_c+\mu\frac{x_2}{R_2^3}=\frac{V_c'}{m_2} \tag{23}$$

$$\omega_1\omega_2 x_2-\left(\omega_1^2+\omega_3^2\right)y_c+\mu\frac{y_c}{R_2^3}=0 \tag{24}$$

$$\left(\omega_1 x_2+\omega_2 y_c\right)\omega_3=0 \tag{25}$$

where $R_1=\|\boldsymbol{R_1}\|$ and $R_2=\|\boldsymbol{R_2}\|$. It is also assumed that $x_1>x_2$ and let $L=x_1-x_2>0$. Further, define $\boldsymbol{R}_c=(x_c,y_c,0)^T$ where $x_c=\left(m_1x_1+m_2x_2\right)/\left(m_1+m_2\right)$. Then the expressions for x_1, x_2 and y_c are $x_1=x_c+m_2L/\left(m_1+m_2\right)$, $x_2=x_c-m_1L/\left(m_1+m_2\right)$ and $y_c=\left[R_c^2-\frac{L^2}{4}\left(\frac{m_1-m_2}{m_1+m_2}\right)^2\right]^{1/2}$.

The relative equilibria of the two craft formation corresponds to solving the equations (20-25) for a given set of values for μ, m_1, m_2, L and $R_c=\|\boldsymbol{R_c}\|$. Reference 15 presents three great circle equilibrium solutions in the context of a spring force acting between two point masses. Since the mathematical development for the restricted two-body system with Coulomb force acting between the two spacecraft point masses is similar to that given in Reference 15 the great circle equilibria results obtained are summarized below (Case 1a-1c). But, for completeness, the non-great-circle equilibria methodology is presented (Case 2).

Setting $\omega_3\neq 0$ in the equilibrium conditions and using $y_c\neq 0$ yield tangential equilibrium solution (Case 1a) and with $\omega_3\neq 0, y_c=0$ gives radial equilibrium solution (Case 1b). Similarly, $\omega_3=0, y_c\neq 0$, and $R_1=R_2$ yields orbit normal equilibrium. And $\omega_3=0, y_c\neq 0, R_1\neq R_2$ gives non-great-circle equilibria (Case 2).

Case 1a. *Tangential Equilibrium* (Figure 5(a))

$$\boldsymbol{R}_1=\left(\tfrac{1}{2}L,y_c,0\right)^T,\ \boldsymbol{R}_2=\left(-\tfrac{1}{2}L,y_c,0\right)^T,\ \boldsymbol{\omega}=(0,0,\omega_3)^T$$
$$y_c=R_c,\ \omega_3^2=\tfrac{\mu}{R^3}\text{ and }V_c'=0.$$

Case 1b. *Radial equilibrium* (Figure 5(b))

$$\boldsymbol{R}_1=(x_1,0,0)^T,\ \boldsymbol{R}_2=(x_2,0,0)^T,\ \boldsymbol{\omega}=(0,0,\omega_3)^T$$
$$\omega_3^2=\tfrac{\mu}{(m_1+m_2)R_c}\left(\tfrac{m_1}{x_1^2}+\tfrac{m_2}{x_2^2}\right)\text{ and }V_c'=\tfrac{\mu m_1m_2\left(x_1^3-x_2^3\right)}{(m_1+m_2)x_1^2x_2^2R_c}>0.$$

Case 1c. *Orbit normal equilibrium* (Figure 5(c))

$$\boldsymbol{R}_1=\left(\tfrac{1}{2}L,y_c,0\right)^T,\ \boldsymbol{R}_2=\left(-\tfrac{1}{2}L,y_c,0\right)^T,\ \boldsymbol{\omega}=(\omega_1,0,0)^T$$
$$m_1=m_2,\ y_c=R_c,\ \omega_1^2=\tfrac{\mu}{R^3},\ V_c'=-\tfrac{\mu m_1L}{2R^3}<0$$

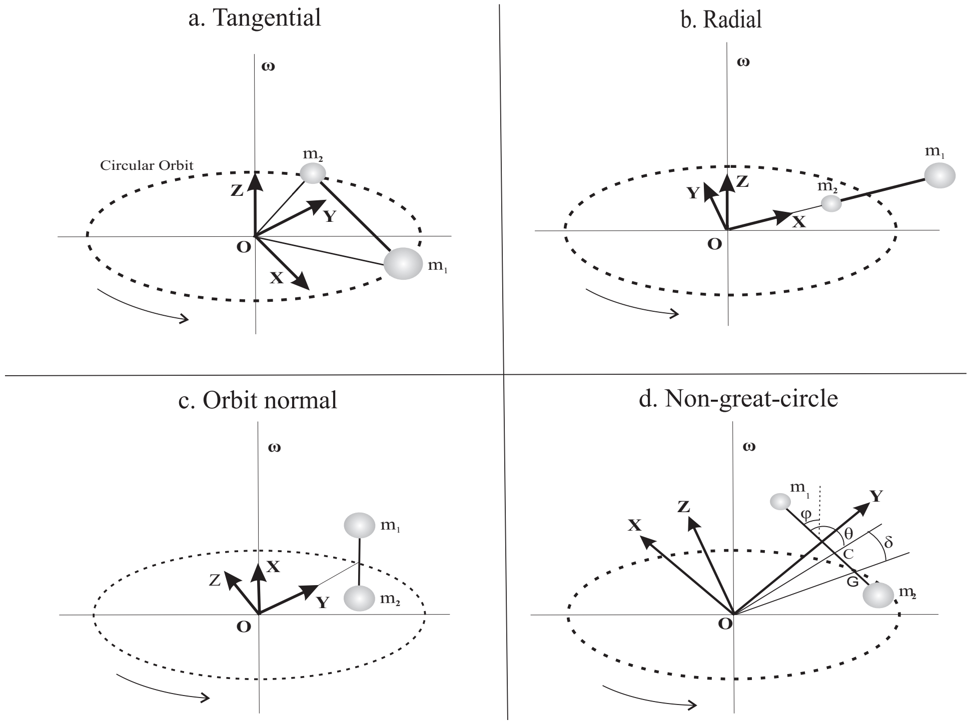

Figure 5. Relative Equilibrium Solutions

Case 2. *Non-great-circle* equilibrium conditions $\omega_3 = 0$, $y_c \neq 0$ and $R_1 \neq R_2$.

With $\omega_3 = 0$, the relative equilibrium equations reduce to

$$-\omega_2^2 x_1 + \omega_1\omega_2 y_c + \mu\frac{x_1}{R_1^3} = -\frac{V_c'}{m_1} \tag{26a}$$

$$\omega_1\omega_2 x_1 - \omega_1^2 y_c + \mu\frac{y_c}{R_1^3} = 0 \tag{26b}$$

$$-\omega_2^2 x_2 + \omega_1\omega_2 y_c + \mu\frac{x_2}{R_2^3} = \frac{V_c'}{m_2} \tag{26c}$$

$$\omega_1\omega_2 x_2 - \omega_1^2 y_c + \mu\frac{y_c}{R_2^3} = 0 \tag{26d}$$

Solving Eqs. (26b) and (26d), we have

$$(x_1 - x_2)\,\omega_1\omega_2 = -\mu y_c\left(\frac{1}{R_1^3} - \frac{1}{R_2^3}\right) \neq 0 \tag{27}$$

which implies that $\omega_1 \neq 0$ and $\omega_2 \neq 0$. Multiplying Eq. (26b) by m_1 and (26d) by m_2 and then adding the resulting equations gives

$$-(m_1 + m_2)(\omega_2 x_c - \omega_1 y_c)\,\omega_1 = \mu\left(\frac{m_1}{R_1^3} + \frac{m_2}{R_2^3}\right) y_c \neq 0 \tag{28}$$

Eq. (28) implies that $(\omega_2 x_c - \omega_1 y_c) \neq 0$. Now, combining Eqs. (26a) and (26c), we obtain

$$(m_1 + m_2)(\omega_2 x_c - \omega_1 y_c)\,\omega_2 = \mu\left(\frac{m_1 x_1}{R_1^3} + \frac{m_2 x_2}{R_2^3}\right) \neq 0 \tag{29}$$

If we define f_x and f_y to be

$$f_x = \frac{m_1 x_1}{R_1^3} + \frac{m_2 x_2}{R_2^3} \neq 0 \tag{30}$$

$$f_y = \left(\frac{m_1}{R_1^3} + \frac{m_2}{R_2^3}\right) y_c \neq 0 \tag{31}$$

The ratio of Eqs. (28) and (29) is

$$\frac{\omega_2}{\omega_1} = -\frac{f_x}{f_y} \tag{32}$$

Also, it can be shown that

$$f_x y_c - f_y x_c = \frac{m_1 m_2}{m_1 + m_2}\left(\frac{1}{R_1^3} - \frac{1}{R_2^3}\right)(x_a - x_b)\, y_c \neq 0 \tag{33}$$

Substituting Eq. (32) into Eq. (33) gives the condition

$$x_c \omega_1 + y_c \omega_2 \neq 0 \tag{34}$$

which is equivalent to $\boldsymbol{R}_c \cdot \boldsymbol{\omega} \neq 0$. This analytically proves that for the given conditions in Case 2b there is no great circle equilibria. Also, in Reference 15, it is shown that non-great-circle equilibria exist only if $m_1 \neq m_2$. Furthermore, with Coulomb formations we can have very lumpy distribution of masses (consider a small camera flying in a fixed location relative to a large mother spacecraft), and thus these non-great-circle equilibria conditions are of interest. Therefore, the non-great-circle equilibrium conditions are

$$\boldsymbol{R}_1 = (x_1, y_c, 0)^T, \boldsymbol{R}_2 = (x_2, y_c, 0)^T, \boldsymbol{\omega} = (\omega_1, \omega_2, 0)^T$$

Eliminating ω_1 and ω_2 from Eqs. (27), (28) and (29) one obtains

$$f = f_x f_1 + f_y f_2 = 0 \tag{35}$$

where $f_1 = \frac{x_2}{R_1^3} - \frac{x_1}{R_2^3}$ and $f_2 = \left(\frac{1}{R_1^3} - \frac{1}{R_2^3}\right) y_c$. The solutions of Eq. (35) provide the non-great-circle equilibria. In order to simplify the solution methodology, Eq. (35) can be expressed in terms of one variable θ, the angle between $\boldsymbol{R}_c$ and x-axis of the rotating frame as shown in Figure 5(d). Therefore let $x_c = R_c \cos(\theta)$ and $y_c = R_c \sin(\theta)$. Plugging in x_c and y_c values into Eq. (35) yields a function of θ. Since $f(\theta)$ is a continuous function for a Coulomb formation ($R_c >> L$) and $f(0) < 0$, $f(\pi) > 0$, there exists a solution for $f(\theta) = 0$. Also as $\frac{df(\theta)}{d\theta} > 0$ it proves that the solution to the equation $f(\theta) = 0$ is unique in the domain $[0, \pi]$. The actual deflection angle, φ, from the vertical can be computed from the angle between x-axis and $\boldsymbol{\omega}$, while $\theta - \varphi$ is the angle between $\boldsymbol{\omega}$ and $\boldsymbol{R}_c$.

Reference 15 discusses the existence of non-great-circle equilibria for long tethers. For spacecraft that are separated by 350 km at LEO a deflection of about 1 degree from the vertical to the orbital plane is observed. For comparison, Table 1 shows the results of $f(\theta) = 0$ for LEO where $R_c =$ 7000 km and $L = 350$ km. The deflection angle φ and error δ are shown in Figure 5(d) where

Table 1. Nongreat-circle relative equilibria at LEO

m_1 (kg)	m_2 (kg)	θ (deg)	φ (deg)	δ (deg)
100	9900	91.052659	1.052684	−0.000026048

the error δ is defined to be $\theta - \varphi - 90°$. The error $\delta \neq 0$ numerically proves the existence of non-great-circle equilibrium for long tethers.

Coulomb formations at GEO are being considered where $R_c = 42,000$ km and the spacecraft's separation distances range from 10 m to 100 m. The current formulation to compute the non-great-circle equilibria is independent of Coulomb formation spacecraft separation distances and can be used to further analyze any separation distance between two spacecraft in formation. The effect of non-great-circle equilibria on two-craft formation formation is studied as a function of spacecraft separation distance L and mass distribution ratio

$$\text{Mass Ratio: } \frac{m_1}{m_1 + m_2}$$

The spacecraft separation distances range from 10 m to 1000 km and formation center of mass distances from LEO to GEO heights. From the contour plots shown in Figure 6, separation distances and mass asymmetry has an effect at LEO heights; however, for Coulomb formation distances at GEO the deflection from normal is less than 10^{-6} degrees and is virtually zero for smaller separation distances, and mass asymmetry also showed negligible effect on the attitude deflection. Even for a case where there is a 10,000:1 mass ratio, the non-great-circle equilibria deflection for geostationary orbits are on the order of 10^{-5} to 10^{-6} degrees. Therefore, the effect of orbit-attitude coupling can be ignored for Coulomb formation separation distances at GEO to search for static Coulomb structure using approximate numerical search algorithms such as evolutionary search strategies.

RELATIVE EQUILIBRIA IN THE RESTRICTED THREE-BODY SYSTEM

In a restricted three-body system, for the Coulomb spacecraft formation with $\boldsymbol{SO}(3)$ symmetry the relative equilibrium is an equilibrium in a uniformly rotating frame. If the vector $\boldsymbol{\xi}$ denotes the angular velocity of the uniformly rotating frame located at barycenter O, the augmented potential for the two spacecraft formation is,

$$\begin{aligned} V_{\xi}\left(\boldsymbol{r_1}, \boldsymbol{r_2}\right) = &-\mu_1 \left(\frac{m_1}{\|\boldsymbol{r_1} - \boldsymbol{d}_1\|} + \frac{m_2}{\|\boldsymbol{r_2} - \boldsymbol{d}_1\|} \right) - \mu_2 \left(\frac{m_1}{\|\boldsymbol{r_1} - \boldsymbol{d}_2\|} + \frac{m_2}{\|\boldsymbol{r_2} - \boldsymbol{d}_2\|} \right) \\ &+ k_c \frac{q_1 q_2}{\|\boldsymbol{r_1} - \boldsymbol{r_2}\|} e^{-\frac{\|\boldsymbol{r_1} - \boldsymbol{r_2}\|}{\lambda_d}} - \frac{m_1}{2} \left\langle \boldsymbol{\xi} \times \boldsymbol{r_1}, \boldsymbol{\xi} \times \boldsymbol{r_1} \right\rangle - \frac{m_2}{2} \left\langle \boldsymbol{\xi} \times \boldsymbol{r_2}, \boldsymbol{\xi} \times \boldsymbol{r_2} \right\rangle \end{aligned} \tag{36}$$

Then the relative equilibria of the system can be characterized by the critical points of the augmented potential V_ξ. The first variation of V_ξ taken component wise with respect to $\boldsymbol{q} = (\boldsymbol{r_1}, \boldsymbol{r_2})$ is computed as

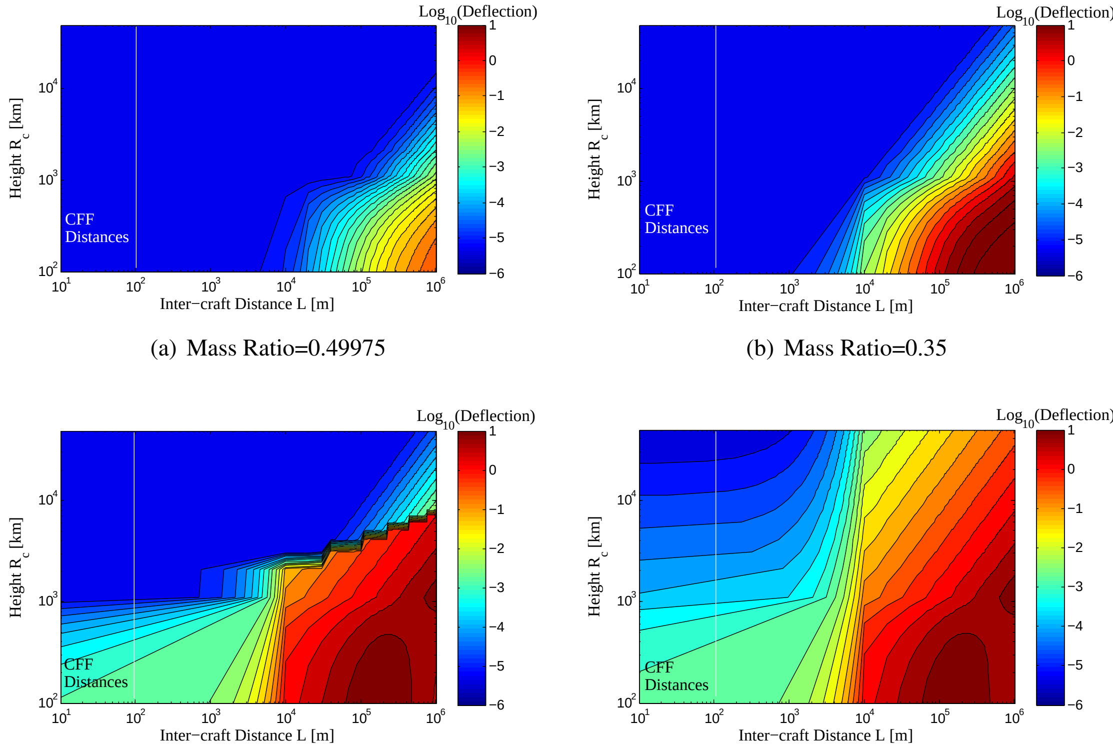

(a) Mass Ratio=0.49975

(b) Mass Ratio=0.35

(c) Mass Ratio=0.05

(d) Mass Ratio=0.0001

Figure 6. Deflection for an Asymmetric Mass Distribution.

$$
\begin{aligned}
\boldsymbol{D}V_{\xi}\left(\boldsymbol{r_1},\boldsymbol{r_2}\right)\cdot\left(\delta\boldsymbol{r_1},\delta\boldsymbol{r_2}\right) = {} & \mu_1 m_1 \frac{\boldsymbol{r_1}-\boldsymbol{d}_1}{\|\boldsymbol{r_1}-\boldsymbol{d}_1\|^3}\cdot\delta\boldsymbol{r_1} + \mu_1 m_2 \frac{\boldsymbol{r_2}-\boldsymbol{d}_1}{\|\boldsymbol{r_2}-\boldsymbol{d}_1\|^3}\cdot\delta\boldsymbol{r_2} \\
& + \mu_2 m_1 \frac{\boldsymbol{r_1}-\boldsymbol{d}_2}{\|\boldsymbol{r_1}-\boldsymbol{d}_2\|^3}\cdot\delta\boldsymbol{r_1} + \mu_2 m_2 \frac{\boldsymbol{r_2}-\boldsymbol{d}_2}{\|\boldsymbol{r_2}-\boldsymbol{d}_2\|^3}\cdot\delta\boldsymbol{r_2} \\
& - k_c \frac{q_1 q_2}{\|\boldsymbol{r_1}-\boldsymbol{r_2}\|^2} e^{-\frac{\|\boldsymbol{r_1}-\boldsymbol{r_2}\|}{\lambda_d}} \left[1+\frac{\|\boldsymbol{r_1}-\boldsymbol{r_2}\|}{\lambda_d}\right] \frac{\boldsymbol{r_1}-\boldsymbol{r_2}}{\|\boldsymbol{r_1}-\boldsymbol{r_2}\|}\cdot\left(\delta\boldsymbol{r_1}-\delta\boldsymbol{r_2}\right) \\
& + m_1\left(\hat{\boldsymbol{\xi}}\hat{\boldsymbol{\xi}}\boldsymbol{r_1}\right)\cdot\delta\boldsymbol{r_1} + m_2\left(\hat{\boldsymbol{\xi}}\hat{\boldsymbol{\xi}}\boldsymbol{r_2}\right)\cdot\delta\boldsymbol{r_2}
\end{aligned}
\tag{37}
$$

Using the expression for $V_c^{'}$ from Eq. (17), Eq. (37) can be expressed as

$$
\begin{aligned}
DV_{\xi}\left(\boldsymbol{r_1},\boldsymbol{r_2}\right)\cdot\left(\delta\boldsymbol{r_1},\delta\boldsymbol{r_2}\right) = {} & \mu_1 m_1 \frac{\boldsymbol{r_1}-\boldsymbol{d}_1}{\|\boldsymbol{r_1}-\boldsymbol{d}_1\|^3}\cdot\delta\boldsymbol{r_1} + \mu_1 m_2 \frac{\boldsymbol{r_2}-\boldsymbol{d}_1}{\|\boldsymbol{r_2}-\boldsymbol{d}_1\|^3}\cdot\delta\boldsymbol{r_2} \\
& + \mu_2 m_1 \frac{\boldsymbol{r_1}-\boldsymbol{d}_2}{\|\boldsymbol{r_1}-\boldsymbol{d}_2\|^3}\cdot\delta\boldsymbol{r_1} + \mu_2 m_2 \frac{\boldsymbol{r_2}-\boldsymbol{d}_2}{\|\boldsymbol{r_2}-\boldsymbol{d}_2\|^3}\cdot\delta\boldsymbol{r_2} \\
& + V_c^{'}\left(\|\boldsymbol{r_1}-\boldsymbol{r_2}\|\right)\frac{\boldsymbol{r_1}-\boldsymbol{r_2}}{\|\boldsymbol{r_1}-\boldsymbol{r_2}\|}\cdot\left(\delta\boldsymbol{r_1}-\delta\boldsymbol{r_2}\right) \\
& + m_1\left(\hat{\boldsymbol{\xi}}\hat{\boldsymbol{\xi}}\boldsymbol{r_1}\right)\cdot\delta\boldsymbol{r_1} + m_2\left(\hat{\boldsymbol{\xi}}\hat{\boldsymbol{\xi}}\boldsymbol{r_2}\right)\cdot\delta\boldsymbol{r_2}
\end{aligned}
\tag{38}
$$

Then setting $DV_\xi\left(\boldsymbol{r_{1e}}, \boldsymbol{r_{2e}}\right) = 0$ leads to the following relative equilibria conditions:

$$\mu_1 m_1 \frac{\boldsymbol{r_{1e}} - \boldsymbol{d}_1}{\|\boldsymbol{r_{1e}} - \boldsymbol{d}_1\|^3} + \mu_2 m_1 \frac{\boldsymbol{r_{1e}} - \boldsymbol{d}_2}{\|\boldsymbol{r_{1e}} - \boldsymbol{d}_2\|^3} + m_1 \hat{\boldsymbol{\xi}}\hat{\boldsymbol{\xi}} \boldsymbol{r_{1e}} + V_c' \frac{\boldsymbol{r_{1e}} - \boldsymbol{r_{2e}}}{\|\boldsymbol{r_{1e}} - \boldsymbol{r_{2e}}\|} = 0 \tag{39a}$$

$$\mu_1 m_2 \frac{\boldsymbol{r_{2e}} - \boldsymbol{d}_1}{\|\boldsymbol{r_{2e}} - \boldsymbol{d}_1\|^3} + \mu_2 m_2 \frac{\boldsymbol{r_{2e}} - \boldsymbol{d}_2}{\|\boldsymbol{r_{2e}} - \boldsymbol{d}_2\|^3} + m_2 \hat{\boldsymbol{\xi}}\hat{\boldsymbol{\xi}} \boldsymbol{r_{2e}} - V_c' \frac{\boldsymbol{r_{1e}} - \boldsymbol{r_{2e}}}{\|\boldsymbol{r_{1e}} - \boldsymbol{r_{2e}}\|} = 0 \tag{39b}$$

The vectors $\boldsymbol{R}_{11}$, $\boldsymbol{R}_{12}$, $\boldsymbol{R}_{21}$ and $\boldsymbol{R}_{22}$ shown in Figure 3 are represented in terms of $\boldsymbol{r_{1e}}$, $\boldsymbol{r_{2e}}$, $\boldsymbol{d}_1$, and $\boldsymbol{d}_2$ as follows

$$\begin{aligned} \boldsymbol{R}_{11} &= \boldsymbol{r_{1e}} - \boldsymbol{d}_1, \qquad & \boldsymbol{R}_{12} &= \boldsymbol{r_{1e}} - \boldsymbol{d}_2 \\ \boldsymbol{R}_{21} &= \boldsymbol{r_{2e}} - \boldsymbol{d}_1, \qquad & \boldsymbol{R}_{22} &= \boldsymbol{r_{2e}} - \boldsymbol{d}_2 \end{aligned} \tag{40}$$

Therefore, Eqs. (39a) and (39b) become

$$\mu_1 m_1 \frac{\boldsymbol{r_{1e}} - \boldsymbol{d}_1}{R_{11}^3} + \mu_2 m_1 \frac{\boldsymbol{r_{1e}} - \boldsymbol{d}_2}{R_{12}^3} \boldsymbol{r_{1e}} + m_1 \hat{\boldsymbol{\xi}}\hat{\boldsymbol{\xi}} \boldsymbol{r_{1e}} + V_c' \frac{\boldsymbol{r_{1e}} - \boldsymbol{r_{2e}}}{\|\boldsymbol{r_{1e}} - \boldsymbol{r_{2e}}\|} = 0 \tag{41a}$$

$$\mu_1 m_2 \frac{\boldsymbol{r_{2e}} - \boldsymbol{d}_1}{R_{21}^3} + \mu_2 m_2 \frac{\boldsymbol{r_{2e}} - \boldsymbol{d}_2}{R_{22}^3} + m_2 \hat{\boldsymbol{\xi}}\hat{\boldsymbol{\xi}} \boldsymbol{r_{2e}} - V_c' \frac{\boldsymbol{r_{1e}} - \boldsymbol{r_{2e}}}{\|\boldsymbol{r_{1e}} - \boldsymbol{r_{2e}}\|} = 0 \tag{41b}$$

where $R_{11} = \|\boldsymbol{R}_{11}\|$, $R_{12} = \|\boldsymbol{R}_{12}\|$, $R_{21} = \|\boldsymbol{R}_{21}\|$ and $R_{22} = \|\boldsymbol{R}_{22}\|$.

Now consider a rotation matrix $[FS] \in \boldsymbol{SO}(3)$ that maps vectors from synodic frame S into a new reference frame F. If we denote the vectors $\boldsymbol{R_1}$, $\boldsymbol{R_2}$, $\boldsymbol{\omega}$ in the reference frame S then the conditions of relative equilibria given in Eqs. 41a and 41b are invariant under the transformation $\boldsymbol{R_1} = [FS]\,\boldsymbol{r_{1e}}$, $\boldsymbol{R_2} = [FS]\,\boldsymbol{r_{2e}}$ and $\boldsymbol{\omega} = [FS]\,\boldsymbol{\xi}$. As illustrated in Figure 7, a reference frame is chosen such that the x-axis is parallel to the line connecting the two crafts, the z-axis being perpendicular to both the vectors $\boldsymbol{r_{1e}}$ and $\boldsymbol{r_{2e}}$, and the y-axis completing the triad. Also, let γ be the angle in the orbit plane between the two frames S and F.

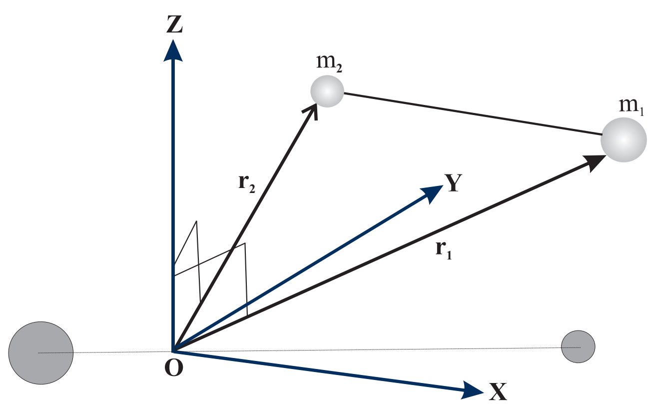

Figure 7. The Rotating Reference Frame (Restricted Three-body System)

In the context of the new frame F, the vectors can be expressed as $\boldsymbol{R}_1 = (x_1, y_c, 0)^T$, $\boldsymbol{R}_2 = (x_2, y_c, 0)^T$, and $\boldsymbol{\omega} = (\omega_1, \omega_2, \omega_3)^T$. The vectors $\boldsymbol{d}_1$ and $\boldsymbol{d}_2$ in the F frame become $(-d_1 \cos\gamma, -d_1 \sin\gamma, 0)$

and $(d_2 \cos\gamma, d_2 \sin\gamma, 0)$. Now the equilibrium conditions (41a) and (41b) expressed in scalar form are,

$$-\left(\omega_2^2+\omega_3^2\right)x_1+\omega_1\omega_2 y_c+\mu_1\left(\frac{x_1+d_1\cos\gamma}{R_{11}^3}\right)+\mu_2\left(\frac{x_1-d_2\cos\gamma}{R_{12}^3}\right)=-\frac{V_c'}{m_1} \tag{42}$$

$$\omega_1\omega_2 x_1-\left(\omega_1^2+\omega_3^2\right)y_c+\mu_1\left(\frac{y_c+d_1\sin\gamma}{R_{11}^3}\right)+\mu_2\left(\frac{y_c-d_2\sin\gamma}{R_{12}^3}\right)=0 \tag{43}$$

$$\left(\omega_1 x_1+\omega_2 y_c\right)\omega_3=0 \tag{44}$$

$$-\left(\omega_2^2+\omega_3^2\right)x_2+\omega_1\omega_2 y_c+\mu_1\left(\frac{x_2+d_1\cos\gamma}{R_{21}^3}\right)+\mu_2\left(\frac{x_2-d_2\cos\gamma}{R_{22}^3}\right)=\frac{V_c'}{m_2} \tag{45}$$

$$\omega_1\omega_2 x_2-\left(\omega_1^2+\omega_3^2\right)y_c+\mu_1\left(\frac{y_c+d_1\sin\gamma}{R_{21}^3}\right)+\mu_2\left(\frac{y_c-d_2\sin\gamma}{R_{22}^3}\right)=0 \tag{46}$$

$$\left(\omega_1 x_2+\omega_2 y_c\right)\omega_3=0 \tag{47}$$

It is also assumed that $x_1 > x_2$ and let $L = x_1 - x_2 > 0$. Further, define $\boldsymbol{R}_c = (x_c, y_c, 0)^T$ where $x_c = (m_1x_1 + m_2x_2)/(m_1 + m_2)$. Then the expressions for x_1, x_2 and y_c are $x_1 = x_c + m_2L/(m_1 + m_2)$, $x_2 = x_c - m_1L/(m_1 + m_2)$ and $y_c = \left[R_c^2 - \frac{L^2}{4}\left(\frac{m_1-m_2}{m_1+m_2}\right)^2\right]^{1/2}$.

The relative equilibria of the two craft formation corresponds to solving the equations (42-47) for a given set of values for μ_1, μ_2, m_1, m_2, L and $R_c = \|\boldsymbol{R_c}\|$. Since there are more number of unknowns to the number of these equations certain constraints are needed in order to find the relative equilibria. For libration point missions, the frame rotates at a constant angular velocity Ω given in Eq. 10. Let us consider angular velocity constraints $\omega_3 = \Omega \neq 0$ (Case 1) and $\omega_3 = 0$ (Case 2).

Case 1. As $\omega_3 \neq 0$ Eq. (44) implies $(\omega_1x_1 + \omega_2y_c) = 0$ and $x_1 \neq 0$ due to the adopted frame which indicates that $\omega_1 = 0$ and $\omega_2y_c = 0$. Using the conditions $\omega_3 \neq 0$ and $\omega_1 = 0$ in equations (43) and (46) and subtracting one from the other gives rise to

$$\left[\mu_1\left(\frac{1}{R_{11}^3}-\frac{1}{R_{21}^3}\right)(y_c+d_1\sin\gamma)+\mu_2\left(\frac{1}{R_{12}^3}-\frac{1}{R_{22}^3}\right)(y_c-d_2\sin\gamma)\right]=0 \tag{48}$$

From Eq. (48), two more conditions arise, $y_c + d_1 \sin\gamma \neq 0, y_c - d_2 \sin\gamma \neq 0$ or $y_c + d_1 \sin\gamma = 0, y_c - d_2 \sin\gamma = 0$. Therefore, the conditions of relative equilibria are further expressed as Case 1a and Case 1b.

Case 1a. $\omega_1 = 0, \omega_3 \neq 0, \omega_2y_c = 0, y_c + d_1 \sin\gamma \neq 0$ and $y_c - d_2 \sin\gamma \neq 0$.

Here $y_c + d_1 \sin\gamma \neq 0$ implies that $y_c \neq 0, \gamma \neq 0$ and forces $\omega_2 = 0$ and Eq. (48) yields $R_{11} = R_{21}$ and $R_{12} = R_{22}$. Applying these conditions to Eqs. (42) and (45) and dividing one over the other results in the conditions

$$(m_1x_1+m_2x_2)=0 \qquad \text{and} \qquad \gamma=90\,\text{degrees} \tag{49}$$

Therefore the equilibrium solutions in the context of a restricted three-body system (circular orbits) are

$$\boldsymbol{R}_1=\left(\tfrac{1}{2}L,y_c,0\right)^T,\ \boldsymbol{R}_2=\left(-\tfrac{1}{2}L,y_c,0\right)^T,\ \boldsymbol{\omega}=(0,0,\Omega)^T$$
$$y_c=R_c,\text{ and } V_c'=-\tfrac{m_1m_2L}{(m_1+m_2)}\left(\left(\tfrac{\mu_1}{R_{11}^3}+\tfrac{\mu_2}{R_{12}^3}\right)-\Omega^2\right)$$

Since $\boldsymbol{R}_c \cdot \boldsymbol{\omega} = 0$, this is a great circle relative equilibrium. However, in the context of restricted three-body system, for any of the collinear libration point it can be shown that $\Omega^2 < \frac{\mu_1}{R_{11}^3} + \frac{\mu_2}{R_{12}^3}$ which implies that $V_c^{'} < 0$ and from Eq. (17) it indicates that the two spacecraft masses must be charged with same polarity. For any of the triangular libration point it can be shown that $\Omega^2 > \frac{\mu_1}{R_{11}^3} + \frac{\mu_2}{R_{12}^3}$ which implies that $V_c^{'} > 0$ and it indicates that the two spacecraft masses must be charged with opposite polarity. For example, Figure 8 shows the tangential equilibrium solutions at a collinear (L_2) and a triangular (L_4) libration points.

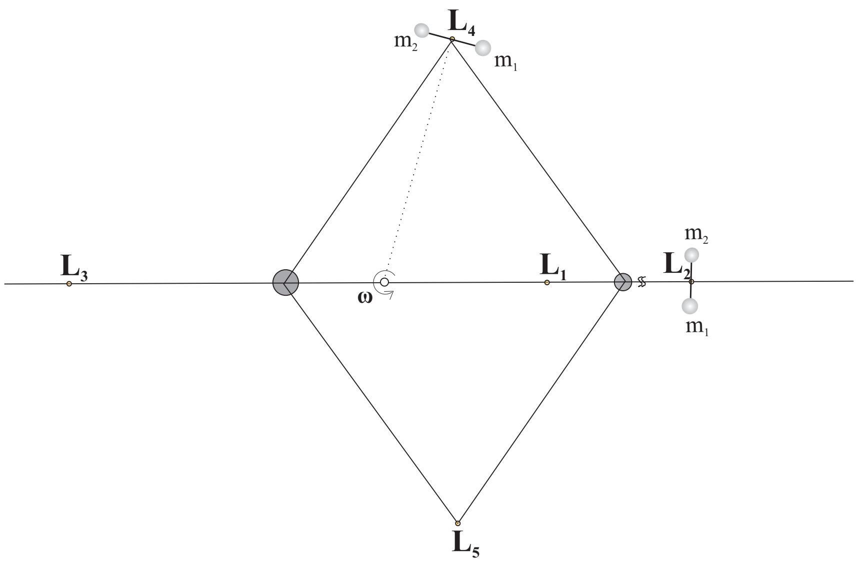

Figure 8. Tangential Relative Equilibrium

Case 1b. $\omega_1 = 0, \omega_3 = \Omega \neq 0, \omega_2 y_c = 0, y_c + d_1 \sin\gamma = 0$ and $y_c - d_2 \sin\gamma = 0$.

It is assumed that $x_1 > x_2 > 0$ for Coulomb formation and as $\omega_3 \neq 0$ and $y_c + d_1 \sin\gamma = 0, y_c - d_2 \sin\gamma = 0$ implies that $y_c = 0, \gamma = 0$ for collinear libration points. However, for Earth-moon triangular libration points $y_c = 0, \gamma = 60.31$ degrees and appropriate values of R_{11}, R_{12}, R_{21} and R_{22} should satisfy Eq. (48). Therefore, for any libration point, from Eq. (44) we can set $\omega_1 = 0$ and $\omega_2 = 0$. With these conditions, Eqs. (42) to (47) reduce to

$$\left(-\Omega^2 + \frac{\mu_1}{R_{11}^3} + \frac{\mu_2}{R_{12}^3}\right) x_1 + \frac{\mu_1 d_1}{R_{11}^3} - \frac{\mu_2 d_2}{R_{12}^3} = -\frac{V_c^{'}}{m_1} \tag{50a}$$

$$\left(-\Omega^2 + \frac{\mu_1}{R_{21}^3} + \frac{\mu_2}{R_{22}^3}\right) x_2 + \frac{\mu_1 d_1}{R_{21}^3} - \frac{\mu_2 d_2}{R_{22}^3} = \frac{V_c^{'}}{m_2} \tag{50b}$$

and solving these equations yields *radial* relative equilibrium with the Coulomb forces directed along the radial axis. The equilibrium solution configuration is

$$\boldsymbol{R}_1 = (x_1, 0, 0)^T, \boldsymbol{R}_2 = (x_2, 0, 0)^T$$

And the expression for $V_c^{'}$ is

$$V_c^{'} = \frac{m_1 m_2}{m_1 + m_2}\left(\Omega^2 L - \mu_1 \left(\frac{1}{R_{11}^3} - \frac{1}{R_{21}^3}\right) - \mu_2 \left(\frac{1}{R_{12}^3} - \frac{1}{R_{22}^3}\right)\right) \tag{51}$$

Since $x_1 > x_2$, from Eq. (40) it can be shown for radial equilibrium that $R_{11} > R_{21}$ and $R_{12} > R_{22}$ for both the collinear and triangular libration points which indicate that $V_c^{'} > 0$. Again $\boldsymbol{R}_c \cdot \boldsymbol{\omega} = 0$, and this is a great circle relative equilibrium as shown in Figure 9. And as $V_c^{'} > 0$ and from Eq. (17) it indicates that the two spacecraft masses must be charged with opposite polarity. This implies that there is a Coulomb force acting between the two masses along the radial direction when the formation is at any of the libration points.

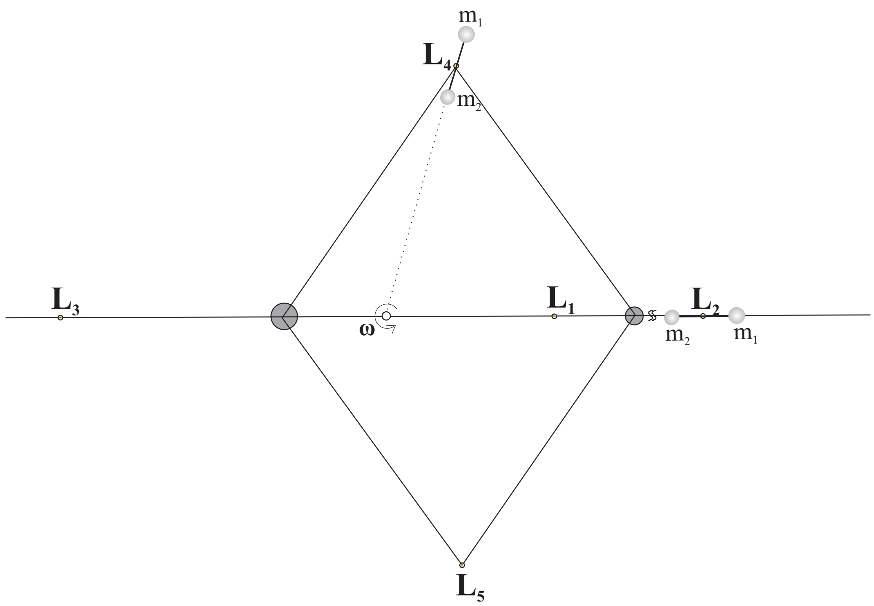

Figure 9. Radial Relative Equilibrium

Case 2. $\omega_3 = 0$. With $\omega_3 = 0$, the relative equilibrium equations reduce to

$$-\omega_2^2 x_1 + \omega_1\omega_2 y_c + \mu_1 \left(\frac{x_1 + d_1\cos\gamma}{R_{11}^3}\right) + \mu_2 \left(\frac{x_1 - d_2\cos\gamma}{R_{12}^3}\right) = -\frac{V_c^{'}}{m_1} \tag{52a}$$

$$\omega_1\omega_2 x_1 - \omega_1^2 y_c + \mu_1 \left(\frac{y_c + d_1\sin\gamma}{R_{11}^3}\right) + \mu_2 \left(\frac{y_c - d_2\sin\gamma}{R_{12}^3}\right) = 0 \tag{52b}$$

$$-\omega_2^2 x_2 + \omega_1\omega_2 y_c + \mu_1 \left(\frac{x_2 + d_1\cos\gamma}{R_{21}^3}\right) + \mu_2 \left(\frac{x_2 - d_2\cos\gamma}{R_{22}^3}\right) = \frac{V_c^{'}}{m_2} \tag{52c}$$

$$\omega_1\omega_2 x_2 - \omega_1^2 y_c + \mu_1 \left(\frac{y_c + d_1\sin\gamma}{R_{21}^3}\right) + \mu_2 \left(\frac{y_c - d_2\sin\gamma}{R_{22}^3}\right) = 0 \tag{52d}$$

Setting $y_c + d_1\sin\gamma = 0$ and $y_c - d_2\sin\gamma = 0$, the equilibrium conditions yield radial equilibrium solutions as seen in Case 1b, but with ω_3 replaced by ω_2. Therefore, we consider only the case where $y_c + d_1\sin\gamma \neq 0$ and $y_c - d_2\sin\gamma \neq 0$. To further study the conditions, we assume that $R_{11} = R_{21}$ and $R_{12} = R_{22}$ (Case 2a) as well as $R_{11} \neq R_{21}$ and $R_{12} \neq R_{22}$ (Case 2b).

Case 2a. $\omega_3 = 0$, $R_{11} = R_{21}$, $R_{12} = R_{22}$, $y_c + d_1\sin\gamma \neq 0$ and $y_c - d_2\sin\gamma \neq 0$.

Using $y_c + d_1\sin\gamma \neq 0$ and $y_c - d_2\sin\gamma \neq 0$ yields $R_{11} = R_{21}$ and $R_{12} = R_{22}$ which gives the condition $x_1 = -x_2$. From Eqs. (52b) and (52d) it implies that $\omega_1 \neq 0$ and we can set $\omega_1 = \Omega$ and

$\omega_2 = 0$. Then, using $x_1 = -x_2$ and $\omega_2 = 0$ in Eqs. (52a) and (52c) yields $m_1 = m_2$ as the only possible condition. As a result the equilibrium solutions obtained are

$$\begin{gathered} \boldsymbol{R}_1 = \left(\tfrac{1}{2}L, y_c, 0\right)^T, \boldsymbol{R}_2 = \left(-\tfrac{1}{2}L, y_c, 0\right)^T, m_1 = m_2, \\ y_c = R_c, V_c' = -\tfrac{m_1 m_2 L}{(m_1+m_2)}\left(\tfrac{\mu_1}{R_{11}^3} + \tfrac{\mu_2}{R_{12}^3}\right) < 0 \end{gathered}$$

These orbit normal equilibrium solutions are applicable for both triangular and collinear libration points with $V_c' < 0$. Specifically, for triangular libration points $R_{11} = R_{21} = R_{12} = R_{22}$ condition holds true. Once again this is a great circle relative equilibrium since $\boldsymbol{R}_c \cdot \boldsymbol{\omega} = 0$. As $V_c' < 0$ and from Eq. (17) it indicates that the two spacecraft masses must be charged with the same polarity. Therefore, there is a Coulomb force acting between the two masses perpendicular to the orbital plane and the two masses are equal and equidistant to the barycenter as shown in Figure 10 at a collinear (L_2) and a triangular (L_4) libration points.

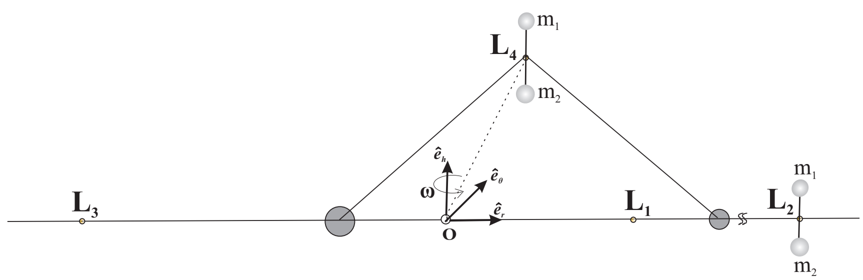

Figure 10. Orbit Normal Relative Equilibrium

Case 2b. $\omega_3 = 0$, $R_{11} \neq R_{21}$, $R_{12} \neq R_{22}$, $y_c + d_1 \sin\gamma \neq 0$ and $y_c - d_2 \sin\gamma \neq 0$.

If we assume that the F frame is aligned with the orbit normal configuration, then $\gamma = 90$ degrees. And, solving Eqs. (52b) and (52d), we have

$$\begin{aligned} -\left(x_1 - x_2\right)\omega_1\omega_2 = y_c &\left(\left(\frac{\mu_1}{R_{11}^3} + \frac{\mu_2}{R_{12}^3}\right) - \left(\frac{\mu_1}{R_{21}^3} + \frac{\mu_2}{R_{22}^3}\right)\right) \\ &+ \mu_1 d_1 \left(\frac{1}{R_{11}^3} - \frac{1}{R_{21}^3}\right) + \mu_2 d_2 \left(\frac{1}{R_{22}^3} - \frac{1}{R_{12}^3}\right) \neq 0 \end{aligned} \tag{53}$$

which implies that $\omega_1 \neq 0$ and $\omega_2 \neq 0$. Now, combining Eqs. (52a) and (52c), we obtain

$$\left(m_1 + m_2\right)\left(\omega_2 x_c - \omega_1 y_c\right)\omega_2 = m_1 x_1 \left(\frac{\mu_1}{R_{11}^3} + \frac{\mu_2}{R_{12}^3}\right) + m_2 x_2 \left(\frac{\mu_1}{R_{21}^3} + \frac{\mu_2}{R_{22}^3}\right) \neq 0 \tag{54}$$

Eq. (54) implies that $(\omega_2 x_c - \omega_1 y_c) \neq 0$. Multiplying Eq. (52b) by m_1 and (52d) by m_2 and then adding the resulting equations gives

$$\begin{aligned} -\left(m_1 + m_2\right)\left(\omega_2 x_c - \omega_1 y_c\right)\omega_1 = &\left(m_1 \left(\frac{\mu_1}{R_{11}^3} + \frac{\mu_2}{R_{12}^3}\right) + m_2 \left(\frac{\mu_1}{R_{21}^3} + \frac{\mu_2}{R_{22}^3}\right)\right) y_c \\ &+ m_1 \left(\frac{\mu_1 d_1}{R_{11}^3} - \frac{\mu_2 d_2}{R_{12}^3}\right) + m_2 \left(\frac{\mu_1 d_1}{R_{21}^3} - \frac{\mu_2 d_2}{R_{22}^3}\right) \neq 0 \end{aligned} \tag{55}$$

If we define f_x and f_y to be

$$f_x = \mu_1 \left(\frac{m_1 x_1}{R_{11}^3} + \frac{m_2 x_2}{R_{21}^3} \right) + \mu_2 \left(\frac{m_1 x_1}{R_{12}^3} + \frac{m_2 x_2}{R_{22}^3} \right) \neq 0 \tag{56}$$

$$\begin{aligned} f_y = & \left(\mu_1 \left(\frac{m_1}{R_{11}^3} + \frac{m_2}{R_{21}^3} \right) + \mu_2 \left(\frac{m_1}{R_{12}^3} + \frac{m_2}{R_{22}^3} \right) \right) y_c \\ & + m_1 \left(\frac{\mu_1 d_1}{R_{11}^3} - \frac{\mu_2 d_2}{R_{12}^3} \right) + m_2 \left(\frac{\mu_1 d_1}{R_{21}^3} - \frac{\mu_2 d_2}{R_{22}^3} \right) \neq 0 \end{aligned} \tag{57}$$

The ratio of Eqs. (54) and (55) is

$$\frac{\omega_2}{\omega_1} = -\frac{f_x}{f_y} \tag{58}$$

Eliminating ω_1 and ω_2 from Eqs. (53), (54) and (55) one obtains

$$f = f_x f_1 + f_y f_2 = 0 \tag{59}$$

where

$$f_1 = x_2 \left(\frac{\mu_1}{R_{11}^3} + \frac{\mu_2}{R_{12}^3} \right) - x_1 \left(\frac{\mu_1}{R_{21}^3} + \frac{\mu_2}{R_{22}^3} \right) + \left(x_2 \left(\frac{\mu_1 d_1}{R_{11}^3} - \frac{\mu_2 d_2}{R_{12}^3} \right) + x_1 \left(\frac{\mu_2 d_2}{R_{22}^3} - \frac{\mu_1 d_1}{R_{21}^3} \right) \right) \frac{1}{y_c}$$

and

$$f_2 = \left(\left(\frac{\mu_1}{R_{11}^3} + \frac{\mu_2}{R_{12}^3} \right) - \left(\frac{\mu_1}{R_{21}^3} + \frac{\mu_2}{R_{22}^3} \right) \right) y_c + \left(\frac{\mu_1 d_1}{R_{11}^3} - \frac{\mu_2 d_2}{R_{12}^3} \right) + \left(\frac{\mu_2 d_2}{R_{22}^3} - \frac{\mu_1 d_1}{R_{21}^3} \right)$$

.

The solutions of Eq. (59) gives the nongreat-circle equilibria and it can be shown that such nongreat-circle equilibria exist only if $m_1 \neq m_2$. Similar to the solution procedure followed for two-body system, Eq. (59) can be expressed in terms of one variable θ, the angle between $\boldsymbol{R}_c$ and x-axis of the rotating frame. Coulomb formation is feasible at the libration points but the spacecraft separation distances range from 10 m to 30 m due to the reduced range of Debye length. The current formulation to compute the nongreat-circle equilibria is independent of Coulomb formation spacecraft's separation distances and can be used to further analyze any separation distance between two spacecraft in formation. The effect of nongreat-circle equilibria on two-craft formation is studied as a function of spacecraft separation distance L and mass distribution ratio

$$\text{Mass Ratio: } \frac{m_1}{m_1 + m_2}$$

The spacecraft separation distances range from 10 m to 10000 km and formation center of mass distances fixed at L_1 and L_2. Figure 11 show the numerical solutions for a range of spacecraft separation distances. For spacecraft separated by more than 9000 km at L_1 and L_2 a deflection of about 1 degree from the vertical to the orbital plane is observed. And, for Coulomb formation distances at L_1 and L_2 the deflection from normal is less than 10^{-6} degrees and is virtually zero for smaller separation distances, and mass asymmetry also showed negligible effect on the attitude deflection. Therefore, the effect of orbit-attitude coupling can be ignored for Coulomb formation separation distances at libration points.

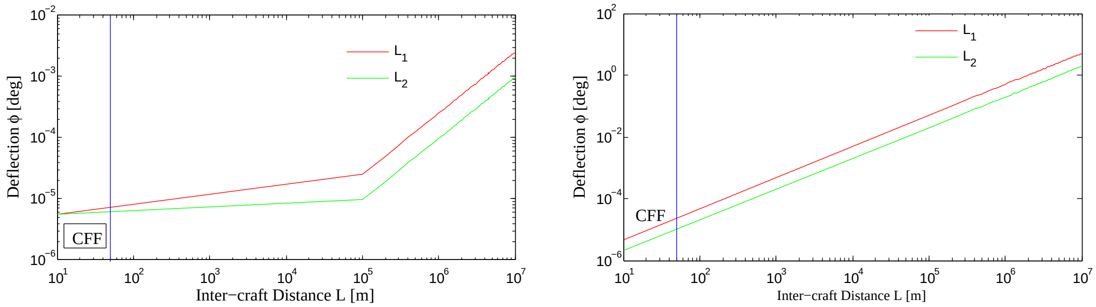

(a) Mass Ratio=0.49975 (b) Mass Ratio=0.0001

Figure 11. Deflection for an Asymmetric Mass Distribution.

CONCLUSION

In this paper, the relative equilibria of a two-craft formation moving in a two-body system and a three-body system are discussed. Previous work has used the simple principle axes condition. The negligible non-great circle effects shown in this paper validates this assumption for Coulomb tether applications. Consequently, for a charged two-craft formation, we conclude that the principal axis condition is very good for genetic algorithms which seek approximate equilibrium answers. However, if one wants to do the full non-linear solutions, these effects can be taken into consideration. Further, for a two spacecraft Coulomb formation moving in a restricted three-body system, this paper presents the relative equilibria at all five libration points. We also numerically show that the non-great circle effects exist for a restricted three-body system and illustrated the results at the L_1 and L_2 collinear libration points. Further, the results obtained in this paper could be used to investigate the linearized dynamics and stability of a 2-craft Coulomb tether formation at libration points.

APPENDIX A. LIE GROUPS

To explain the terminology used in this paper, basic properties and definitions of Lie Groups are introduced here. For a thorough presentation of these concepts refer.[18]

Definition 1 [Group of transformations]. A group of transformations G is an aggregate set of transformations g_i such that the following properties are satisfied:

i) It contains the identity transformation.
ii) Corresponding to each transformation g_l there is an inverse transformation g_l^{-1}.
iii) The composition of transformations holds $g_l g_k \in G$ and the associativity rule $(g_i g_j)\, g_k = g_i\,(g_j g_k)$ is satisfied.

For instance, the set of nonsingular linear transformation matrices forms a group as all the above three properties are satisfied. Another important example is the symmetry group of a rigid body. To maintain the symmetry of a rigid body, symmetry groups or symmetry transformations gives rise to the set of all distance preserving transformations which transforms the position of the body but preserves the distance between all pairs of points of the rigid body.

Definition 2 [Lie group]. A Lie group is a smooth manifold G that has a group structure consistent with its manifold structure such that the group operation and its inversion are smooth maps between manifolds. A matrix representing a rotation about an axis through an angle is an example of a Lie group. The three-dimensional rotation group $\boldsymbol{SO}(3)$ is defined as

$$\boldsymbol{SO}(3) = \left\{ \boldsymbol{C} : \mathbf{R^3} \to \mathbf{R^3} \ \ linear, \ \ \boldsymbol{C}^T \boldsymbol{C} = E \ \ and \ \ det\, \boldsymbol{C} = 1 \right\}$$

Lie groups describe continuous symmetries in physical systems using its Lie algebra $\boldsymbol{g^*}$ for its calculations. Lie algebra is a vector space and uses linear algebra to study Lie groups. For example, $\boldsymbol{SO}(3)$ is a Lie group and can be characterized by its Lie algebra. A Lie group G and its Lie algebra $\boldsymbol{g^*}$ are related similar to the way a flow and the associated vector field are related. The corresponding vector field $\boldsymbol{v}$ on a flow $\boldsymbol{\Phi}\left(\boldsymbol{x}, t\right)$ given by

$$\boldsymbol{v}\left(\boldsymbol{x}\right) = \frac{d}{dt}|_{t=0} \boldsymbol{\Phi}\left(\boldsymbol{x}, t\right),$$

is called the infinitesimal generator of the flow.

Let $\boldsymbol{so}(3)$ be the set of skew-symmetric matrices defined by

$$\boldsymbol{so}(3) = \left\{ \hat{\boldsymbol{\xi}} : \mathbf{R^3} \to \mathbf{R^3}, \ \ linear \ \ \left| \hat{\boldsymbol{\xi}} + \hat{\boldsymbol{\xi}}^T \right| = 0 \right\}$$

where $\boldsymbol{\xi} = (\xi_1, \xi_2, \xi_3)$ is a vector and $\hat{\boldsymbol{\xi}}$ is

$$\left[\hat{\boldsymbol{\xi}}\right] = \begin{bmatrix} 0 & -\xi_3 & \xi_2 \\ \xi_3 & 0 & -\xi_1 \\ -\xi_2 & \xi_1 & 0 \end{bmatrix}$$

This set $\boldsymbol{so}(3)$ forms the Lie algebra of $\boldsymbol{SO}(3)$ given as $\hat{\boldsymbol{\xi}}\boldsymbol{r} = \boldsymbol{\xi} \times \boldsymbol{r}$ for any $\boldsymbol{r} \in \mathbf{R^3}$. If we define the Lie algebra isomorphism between the space $\mathbf{R^3}$ and $\boldsymbol{so}(3)$ by $\boldsymbol{\xi} \mapsto \boldsymbol{so}(3)$ then the matrix exponential $e^{\hat{\boldsymbol{\xi}}t}$ is a rotation about $\boldsymbol{\xi}$ by the angle $\|\boldsymbol{\xi}\|\, t$ in the form

$$\boldsymbol{C}\left(t\right) = e^{\hat{\boldsymbol{\xi}}t}.$$

REFERENCES

[1] King, L. B., Parker, G. G., Deshmukh, S., and Chong, J.-H., ”Spacecraft Formation-Flying using Inter-Vehicle Coulomb Forces,” Tech. rep., NASA/NIAC,January 2002, http://www.niac.usra.edu.

[2] King, L. B., Parker, G. G., Deshmukh, S., and Chong, J.-H., ”Study of Interspacecraft Coulomb Forces and Implications for Formation Flying,” *AIAA Journal of Propulsion and Power*, Vol. 19, No. 3, MayJune 2003, pp. 497505.

[3] Schaub, H., Parker, G. G., and King, L. B., ”Challenges and Prospect of Coulomb Formations,” *AAS John L. Junkins Astrodynamics Symposium, College Station*, TX, May 23-24 2003, Paper No. AAS-03-278.

[4] Parker, G. G., Passerello, C. E., and Schaub, H., ”Static Formation Control using Interspacecraft Coulomb Forces,” *2nd International Symposium on Formation Flying Missions and Technologies*, Washington D.C., Sept. 1416, 2004.

[5] Mullen, E. G., Gussenhoven, M. S., and Hardy, D. A., ”SCATHA Survey of High-Voltage Spacecraft Charging in Sunlight,” *Journal of the Geophysical Sciences*, Vol. 91, 1986, pp. 10741090.

[6] Schaub, H., Hall, C. D., and Berryman, J., ”Necessary Conditions for Circularly-Restricted Static Coulomb Formations,” *AAS Journal of Astronautical Sciences*, Vol 54, No. 3-4, July-Dec 2006, pp 525-541.

[7] Berryman, J., and Schaub, H., ”Analytical Charge Analysis for 2- and 3-Craft Coulomb Formations,” *AIAA Journal of Guidance, Control and Dynamics*, Vol. 30, No. 6, Nov.-Dec. 2007, pp. 1701-1710.

[8] Vasavada, H., and Schaub, H., ”Analytic Solutions for Equal Mass 4-Craft Static Coulomb Formation,” *Journal of Astronautical Sciences*, Vol. 56, No. 1, January-March 2008, pp. 7-40.

[9] Berryman, J., and Schaub, H. ”Static Equilibrium Configurations in GEO Coulomb Spacecraft Formations,” *AAS/AIAA Space Flight Mechanics Meeting*, Copper Mountain, CO, Jan. 23-27, 2005. Paper No. 05-104.

[10] Schaub, H., and Junkins, J. L., ”Analytical Mechanics of Space Systems,” *AIAA Education Series*, Reston , VA , 2003.

[11] Vasavada, H., ”Four Craft Virtual Coulomb Structure Analysis for 1 to 3 Dimensional Geometries,” Master’s Thesis, Aerospace and Ocean Engineering Department, Virginia Polytechnic Institute and State University, Blacksburg, VA, May 2007.

[12] Berryman, J., ”Analytical and Numerical Analysis of Static Coulomb Formations,” Master’s Thesis, Aerospace and Ocean Engineering Department, Virginia Polytechnic Institute and State University, Blacksburg, VA, December 2005.

[13] Natarajan, A., ”A Study of Dynamics and Stability of Two-Craft Coulomb Tether Formations, *Ph.D. Dissertation*, Aerospace and Ocean Engineering Department, Virginia Polytechnic Institute and State University, Blacksburg, VA, May 2007.

[14] Wang, L. S., Maddocks, J.H., and Krishnaprasad, P.S., ”Steady Rigid-Body Motions in a Central Gravitational Field,” *Journal of the Astronautical Sciences*, Vol.40, No.4, 1992, pp.449-478.

[15] Cheng, S. F, and Li-Sheng Wang, L. S, ”Relative equilibria and stabilities of spring-connected bodies in a central gravitational field,” *Celestial Mechanics and Dynamical Astronomy*, Volume 63, Numbers 3-4, September 1995, pp. 289-312.

[16] Beck, J.A., ”Relative Equilibria of a Rigid Satellite in a Central Gravitational Field, *Ph.D. thesis, Air Force Institute of Technology*, Wright-Patterson AFB, OH, Sept. 1997, aFIT/DS/ENY/97-6.

[17] Misra, A. K., Bellerose, J., and Modi, V. J., ”Dynamics of a Tethered System near the Earth-Moon Lagrangian Points,” *Proceedings of the 2001 AAS/AIAA Astrodynamics Specialist Conference*, Quebec City, Canada, Vol. 109 of Advances in the Astronautical Sciences, 2002, pp. 415435.

[18] Marsden, J.E. and Ratiu, T.S., *An Introduction to Mechanics and Symmetry, A Basic Exposition of Classical Mechanical Systems*, Springer-Verlag, New York, Heidelberg, Berlin, 1994.